

Fabrication and Integration of a Low-cost 3D Printing-based Glucose Biosensor for Bioprinted Liver-on-a-chip

Jaehee Lee¹, Somnath Maji¹, and Hyungseok Lee¹

¹Kangwon National University

April 7, 2023

Abstract

In the last two decades, there have been significant advancements in the development of more physiologically relevant organ-on-a-chip (OOC) systems that can mimic the tissue microenvironment. Despite the advantages of these microphysiological systems, such as portability, the ability to mimic physiological flow conditions, and the reduction of reagents required for preparation and detection, they lack real-time detection of analytes with high accuracy. To address this, biosensor technologies have been integrated with OOC systems to enable simultaneous analysis of different analytes in a single device. However, integrating biosensors with OOC systems is challenging due to the competing demands for low-cost, simple fabrication processes, and speed. This study presents the fabrication of a glucose sensing device integrated with a liver-on-a-chip (LOC) platform. The conductive PLA-based three-electrode system was printed using FDM 3D printing technology to simplify the fabrication process. The sensitivity of the glucose biosensing device was enhanced by adding multi-walled carbon nanotubes on the electrodes. The biosensing integration study using a perfusion-based LOC showed the stability, biocompatibility, and sensitivity of the glucose sensing devices. Furthermore, drug toxicity studies on the LOC platform demonstrated the device's ability to detect a broad range of glucose concentrations and its enhanced sensitivity.

1. Introduction

Multidisciplinary research in cell biology and bioengineering over the past two decades has resulted in the development of highly effective in-vitro cell culture platforms that allow the representation of micro-environmental signals (1). As a result, increasingly sophisticated systems that can better represent the essential characteristics of cellular microenvironments are replacing traditional in-vitro models in cell biology systems (2, 3). In this context, the concept of organ-on-a-chip (OOC) has been developed and has been rapidly popularized in the last decade as it can effectively mimic the structure and functional response of human organs (4-7). As such, OOC systems are often considered a substitute for animal-testing studies in cell biology as animal-based pharmaceutical studies often fail to anticipate human pathophysiology (8, 9). However, OOC cell culture analysis is mainly performed using conventional instruments, such as optical measurement methods employing microscopy in conjunction with different staining techniques and the collection of supernatants and cellular samples (10, 11). These conventional methods are labor-intensive, necessitate manual sample collection from the microfluidic system, require high working volumes, and are susceptible to system disruption. Label-free, continuous real-time monitoring of cell functionality is an important technical problem encountered in OOC development.

Several review articles have advocated for the integration of functional tools and sensors within the OOC device for performing real-time cell monitoring. In this regard, numerous methods enabling real-time monitoring without impairing the functionality of OOCs have been proposed in recent years (12-17). High-cost microsensors have also been incorporated (18). Zhang et al. recently developed an automated in-situ monitoring platform for the biophysical (pH, oxygen, and temperature) and biochemical parameters of liver-on-a-chip (LOC) and heart-on-a-chip model systems (19). Sensors have been placed on the device's top, bottom,

and cell culture regions without impairing the device's performance (18, 20-22). To realize optical imaging, impedance monitoring, and metabolite sensing of live kidney cells, Curto et al. employed organic electrochemical transistors along with microfluidics (23). These sensor components were installed at the system's glass bottom cover by using traditional microtechnology methods and the multistep lithography process in clean rooms. Such sensor integration methods pose challenges in fabrication as requirements such as the use of functionally acceptable materials, low production costs, and simplicity and speed of manufacturing must be considered.

Three-dimensional (3D) printing is a simple, quick, low-cost, and adaptable printing process that is becoming increasingly popular as a manufacturing strategy in several research domains (24-26). Fused deposit molding (FDM)-based 3D printing is suitable for fabricating integrated electrochemical sensors as it offers greater options in terms of material selection and increased flexibility in designing and fabricating sensors in terms of size and geometry. The 3D printing technology is based on open-source software, which ensures design portability between 3D systems and enables quick prototyping, high fabrication speed, low operational cost, high precision, and uniformity (minimal batch-to-batch variation). Low-cost conductive plastic 3D-printed materials have been used for electrode fabrication for electrochemical sensing of ascorbic acid, picric acid, catechol, dopamine, Zn (II), and Pb (II) (27-31). However, plastic electrodes have been rarely used as sensing platforms integrated with the OOC system.

We established a 3D-printed conductive polylactic acid (PLA) (CP)-based three-electrode sensing system to serve as an integrated amperometric glucose biosensor for the LOC platform. Glucose is an important regulatory parameter influencing cell growth and functions; in addition, it is a clinical indicator of diabetes. The designed glucose biosensor comprises three electrodes: a working electrode (WE) that reacts directly with the solution, a reference electrode (RE) for comparison with the WE, and a counter electrode (CE) for completing the electrical circuit. Generally, electrodes such as Ag/AgCl and platinum are used because the RE should have little current flow, and the CE should not react with the electrolyte. However, manufacturing these electrodes is time-consuming and expensive. In addition, all three electrodes must be integrated into a single material for realizing simple integrated devices. Although in a previous study, glucose detection has been performed based on the catalytic activity of glucose oxidase (GOx) absorbed from the surface of Nafion-coated CP electrodes (32), we further took the liberty to investigate the sensitivity of the existing three-electrode sensing system by coating an additional layer of multi-walled carbon nanotube (MWCNT). MWCNTs have been extensively studied for their excellent electrical properties (33, 34). Chemically modifying the electrode surface by using carbon nanotubes (CNTs) increases the activity of the electrodes when reacting with physiologically active species such as hydrogen peroxide, hydrazine, dopamine, cholesterol, and NADH (35). The direct adsorption of large biomolecules onto the surface of immobilized MWCNT may help achieve a direct electrical connection between support electrodes and the active site of redox enzymes, thus augmenting the sensitivity of three-electrode biosensors. Integrated glucose biosensors can be assembled onto the LOC platform containing three holders, allowing the flexibility of easy placement and removal of the three-electrode system as per the experimental requirements. We developed a liver in-vitro model by using a coaxial 3D extrusion bioprinter using hepatocellular carcinoma (HepG2) as the cell source. Therefore, in this study, we established a LOC platform with integrated CP biosensors capable of measuring glucose through the coating of Nafion/MWCNT/GOx.

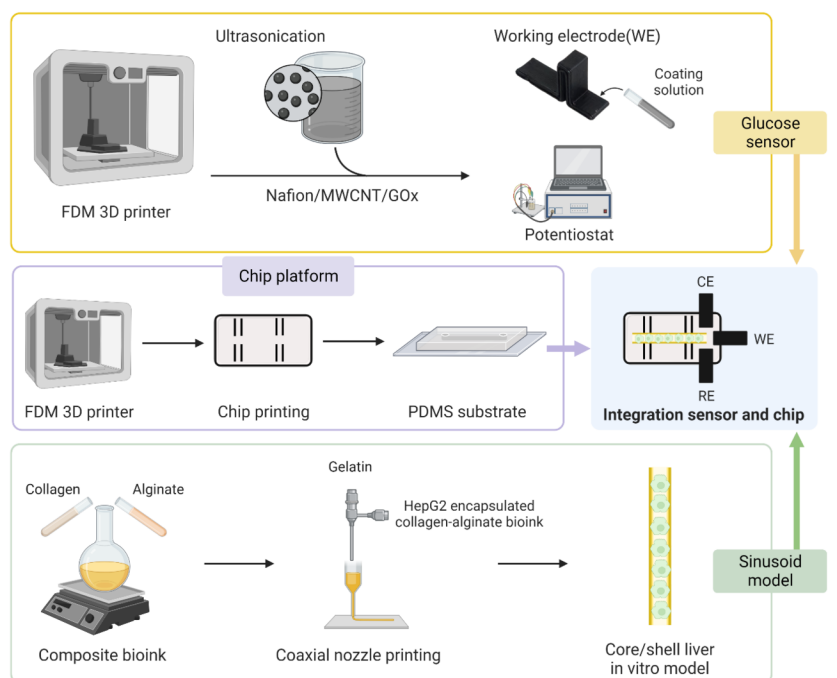


Figure 1. Schematic diagram of the integration process of glucose biosensor and liver-on-a-chip. Figure created with Biorender.com

2. Materials and methods

2.1. Design and printing of conductive PLA

Conductive PLA filaments (diameter: 1.75 mm) were procured from Proto-Pasta (USA), and nonconductive PLA filaments (diameter: 1.75 mm) were obtained from eSUN (China). A dual-printing-head 3D printer (Creator pro 2, Flashforge, China) was used to fabricate the electrodes and other test parts. Computer-aided design of the electrode parts was performed using Solidworks 2020 (Dassault, France) and stored as stereolithography (.stl) files, and the detail printing conditions were adjusted using FlashPrint 5 (Flashforge, China) (nozzle temperature: 215°C, bed temperature: 60°C, printing speed: 60 mm/s, moving speed: 100 mm/s).

2.2. Manufacturing of glucose biosensors

The glucose biosensor was fabricated by coating the printed conductive PLA with GOx solution. Nafion and GOx were purchased from Sigma (USA), and GOx was stored at -20degC until used. Nafion 117 (5% (w/w) in mixed alcohols) was obtained from Sigma (USA). The GOx solution was prepared by dissolving 1X phosphate buffer saline (PBS) at a concentration of 7.2 mg/mL. Nafion/MWCNT solution was prepared by adding 1% (w/v) MWCNT to the Nafion solution. For complete dispersion of MWCNT in the solution, ultrasonication was performed for 30 min, followed by high-speed stirring (800 rpm) at 40degC for 24 h. The produced GOx solution and the Nafion/MWCNT solution were mixed in a 1:1 ratio to prepare the Nafion/MWCNT/GOx solution. To coat the WE, approximately 10 μ L of the Nafion/MWCNT/GOx solution was casted on the part that touches the solution of the printed conductive PLA and incubated at room temperature until the casted solution dried completely.

2.3. SEM analysis of glucose biosensors

Particle morphologies were observed through scanning electron microscopy (SEM; JSM-7900F, JEOL, Japan). To obtain SEM images, all the samples were printed in the same manner (electrode printing

described in Section 2.1) and coated with Nafion, Nafion/MWCNT, and Nafion/MWCNT/GOx solutions. Subsequently, the samples were dried at room temperature and then measurements were performed.

2.4. Preparation of standard solution and electrochemical measurement of glucose biosensors

Glucose standard solutions with concentrations of 1, 3, 10, 50, and 100 mM were prepared and stored in a refrigerator at 37.5°C before performing the electrochemical measurement. The RE, CE, and WE were connected to a potentiostat (WizECM-1200 premium, Wizmac, Korea), and the cyclic voltammetric (CV) and chronoamperometric (CA) measurements were performed at room temperature. CV measurements indicated the oxidation and reduction of glucose and were performed at a scan rate of 100 mV·s⁻¹ for the potential range between -1.0 and +1.0 V. CA measurements were performed for 20 s at regular intervals of 3 s at a detection potential of +0.6V for various glucose concentrations, such as 1, 3, 10, 50, and 100 mM.

2.5. Biocompatibility and 3D cell culture test of glucose biosensors

Human hepatic carcinoma cells (HepG2 cells) were purchased from ATCC, USA and maintained in Dulbecco's modified Eagle's medium (DMEM) supplemented with 10% fetal bovine serum and 1% penicillin under standard cell-culture conditions (i.e., 37degC, 5% CO₂atmosphere). The medium was changed every 3 days. For the experimental study, the cells were trypsinized and subcultured in 48 well plates (1 x 10⁶ cells/mL) per well. The electrodes were autoclaved and coated with the Nafion/MWCNT/GOx solution and then dried at room temperature. The dried coated electrodes were submerged in a well containing attached HepG2 cells, and the setup was incubated for 1, 3, and 7 days. The viability of HepG2 cells was determined using live/dead assays with the staining of calcein-AM and ethidium homodimer. The images were captured using a fluorescence microscope (Nikon, Japan). The hydrogel used in the 3D hydrogel test was prepared using a glass slide and cover slip by mixing alginate and collagen in the 1:1 ratio, and HepG2 cells were encapsulated therein. Approximately 300 µL of the hydrogel was added, and the coverslip was immediately placed on the hydrogel. Then, CaCl₂ was slowly added so that the entire glass slide got submerged in the CaCl₂ solution. If the coverslip got displaced after 2 h, the disc-shaped hydrogel formation was considered completed on the glass slide. For performing the cell glucose consumption test in the 3D hydrogel, HepG2 cells were cultured (2 × 10⁶ cells/mL) inside the hydrogel and cultured in an incubator under standard cell-culture conditions (i.e., 37°C, 5% CO₂ atmosphere). The sample was electrically measured using a w/ cell sample containing cells and a blank sample containing no cells.

2.6. Fabrication of Liver-on-a-chip

The dual extruder Flashforge 3D printer was used to fabricate the PLA-based LOC platform. The chip platform was designed using Solidworks (Dassault) (Figure 1). To print the LOC platform, PLA was loaded into the thermosensitive extruder and printing was performed at a nozzle temperature of 220°C. A core/shell liver 3D in-vitro model was developed using a pneumatic in-house-developed extrusion bioprinter. A polymeric formulation of collagen–alginate composite bioink was used for the encapsulation of HepG2 cells. The composite bioink was prepared by uniformly mixing equal volumetric ratios of collagen (15 mg/mL) and alginate (40 mg/mL). Cell printing of the core/shell liver in-vitro model was performed using a coaxial nozzle connected to two syringes of the bioprinter. HepG2 (2 × 10⁶ cells/mL)-encapsulated collagen–alginate bioink was loaded in the syringe connected to the outer nozzle, whereas the syringe containing 3% gelatin bioink was connected to the inner nozzle. By using a printing code and optimized printing parameters (speed: 200 mm/min, outer pressure: 55 MPa, inner pressure: 55 MPa), the hydrogel was extruded into a lumen-based structure with HepG2-based collagen–alginate bioink on the outer region and gelatin bioink on the core region. The printed structure was crosslinked with CaCl₂.

2.7. Culture condition of Liver-on-a-chip

After the fabrication process, a hepatocyte culture medium was added to the LOC platform. The LOC was incubated at 37°C for 24 h to allow the dissolution of sacrificial bioink (3% gelatin) from the core region of the bioprinted construct. The LOC setup was then transferred onto a rocker cultured at 37°C in a humidified 5% CO₂atmosphere. The free movement of the medium through the hollow lumen of the 3D model simulating

a perfusion-based liver in-vitro model was driven by gravity-induced force. The flow rate (Q) of the medium was calculated using Eqs. (1) and (2):

$$\Delta P = \rho g \Delta h, \quad (1)$$

$$Q = \Delta P \pi R^4 / 8 \mu L, \quad (2)$$

where ΔP , ρ , g , and Δh denote the pressure, fluid density, gravity constant, and height difference ($L \times \sin [10^\circ]$), respectively. ΔP , R , μ , and L denote the pressure drop, hydraulic radius of the channel, dynamic fluid viscosity ($0.78 \times 10^{-3} \text{ Pa}\cdot\text{s}$), and length of the channel (20 mm), respectively. The lumen-based 3D liver microphysiological system had a flow rate of 25 $\mu\text{l}/\text{min}$. Every two days, the culture-related media were replaced.

2.8. Biological characterization of LOC

The proliferation of hepatocytes in the LOC platform was determined using a cell counting kit (CCK-8, Dojindo, Korea). WST-8 solution was added to the culture medium containing the 3D liver sinusoid model. The medium was then incubated for 2 h at 37°C in a humidified 5% CO_2 environment. The absorbance at 450 nm was recorded after 100 μL of the solution was transferred to a 96-well plate.

2.9. Preparation of glucose sensor-integrated in-vitro model

The 3D-printed CP electrodes were assembled by placing the enzyme-casted side of the electrodes inside the chip platform. The 3D-printed CP electrodes were designed such that they could be easily locked in with the chip platform. All three electrodes (WE, CE, and RE) were assembled on the outer chambers of the LOC platform, thereby avoiding any disturbances to the central chamber of the chip that houses the liver sinusoidal in-vitro model. To perform CV and CA measurements, the tail ends of the electrodes were connected to the potentiostat (WizECM-1200 premium, Wizmac, Korea).

2.10. Drug screening analysis and biosensor sensitivity study

The drug toxicity of the LOC platform was determined by incubating it with different concentrations of diclofenac (DF) (1, 10, 100, 200, 400, 800, and 1000 μM) (Sigma) for 48 h. After treatment, the cell viability of the LOC was assessed using the CCK-8 assay, and measurements were performed calorimetrically. To determine the biosensor sensitivity, CA measurement of the drug-treated LOC was performed.

2.11. Statistical analysis

All data were expressed as mean \pm standard deviation. Student's two-tailed t test was used to compare the differences among selected groups. Differences among samples were considered statistically significant at $p < 0.05$.

3. Results and discussion

3.1. Surface coating of 3D-printed working electrode

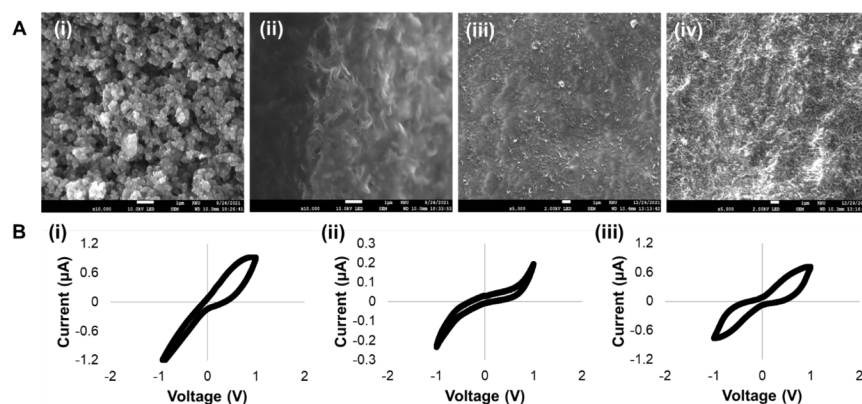


Figure 2. (A) Surface morphology of electrodes with different coating materials studied using scanning electron micrography. The SEM of (i) Bare CP, (ii) Nafion-coated CP, (iii) Nafion/MWCNT-coated CP, and (iv) Nafion/MWCNT/GOx-coated CP. (B) Investigation of variations in cyclic voltammetry graphs based on the electrode coating material: (i) Nafion, (ii) Nafion/GOx, (iii) Nafion/MWCNT/GOx.

A glucose-sensing system using a three-electrode method was developed to measure the concentration of glucose by comparing the reaction of current flowing through the WE and the CE with the RE. Depending on the material and coating of the electrode, the potential at which the enzyme and the solution reacted in the WE varied (36). In addition, the sensitivity and selectivity of the sensor were determined. The design of the WE and the degree of coating of the surface are important. The surface SEM images of the WE with the bare, Nafion, Nafion/MWCNT, and Nafion/MWCNT/GOx coating solutions for the 3D-printed CP electrode for the glucose biosensor are shown in Fig. 2A. As can be seen in Fig. 2A(i), when the CP electrode was not treated, the surface was non-uniform and had sparse holes. As can be seen in Fig. 2A(ii), Nafion was uniformly coated on the surface of the electrode and served as a protective film. MWCNT grains attached gradually (Fig. 2A(iii)), and MWCNT and GOx adhered well to the electrode surface (Fig. 2A(iv)), causing an oxidation–reduction reaction in the electrode well. As can be seen in the CV diagrams of Nafion, Nafion/GOx, and Nafion/MWCNT/GOx coating solutions (Fig. 2B), in the electrode coated with only Nafion, a reduction reaction did not occur well. In contrast, in the CV graph of the electrode coated with Nafion/GOx, an oxidation–reduction reaction occurred continuously; however, a clear oxidation–reduction peak was not observed. As can be seen from the CV graph of the electrode coated with Nafion/MWCNT/GOx to which MWCNT was added, a clear oxidation peak was observed at around ± 0.6 V, indicating that the solution and enzyme were well oxidized and reduced at around ± 0.6 V. Moreover, the functioning of the glucose sensor was checked by measuring the peak at a potential of 0.6 V, as usually measured in conventional electrochemical glucose biosensors (37).

3.2. CA response of the 3D-printed CP electrode

The optimized Nafion/MWCNT/GOx coating solution was applied to the CP electrode. CA measurements were performed at +0.6 V (where the oxidation current starts) for coated and dried electrodes. The CA graph at +0.6 V for different glucose concentrations is depicted in Fig. 3A. Glucose was measurable over a wide range of concentrations (1–100 mM), including 2–40 mM, which is the general blood sugar level. Successful measurements over the range of 1–100 mM indicated that measurements around 1 mM can be performed as well, which is the glucose level of body fluids such as sweat and saliva (38).

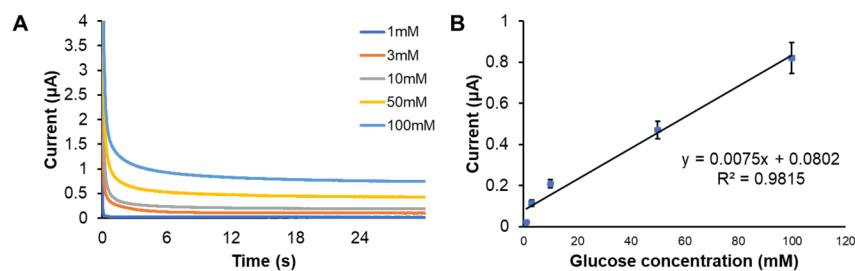


Figure 3. (A) Chronoamperometric response of the 3D-printed CP electrode for increasing glucose concentration (1–100 mM). (B) Corresponding calibration curve measured for increasing glucose concentration (1–100 mM).

Furthermore, as the glucose level of the cell culture medium has a range of 4.5 g/L (~25 mM), the 3D-printed glucose sensor designed in this study can respond to glucose changes in the culture medium while culturing and testing. As can be seen from Fig. 3B, the CA graphs for CP electrodes coated with Nafion/MWCNT/GOx were linear for glucose measurements in the range of 1–100 mM (squared correlation coefficient $R^2 = 0.9813$). The correlation between glucose concentration and current was demonstrated by the linear results for different glucose concentrations by averaging currents from 3–30 s, thus indicating that the designed 3D sensor has a stable measurement potential for glucose concentrations of 1–100 mM.

3.3. Cytotoxicity test of 2D cell culture and glucose readout test of 3D cell culture

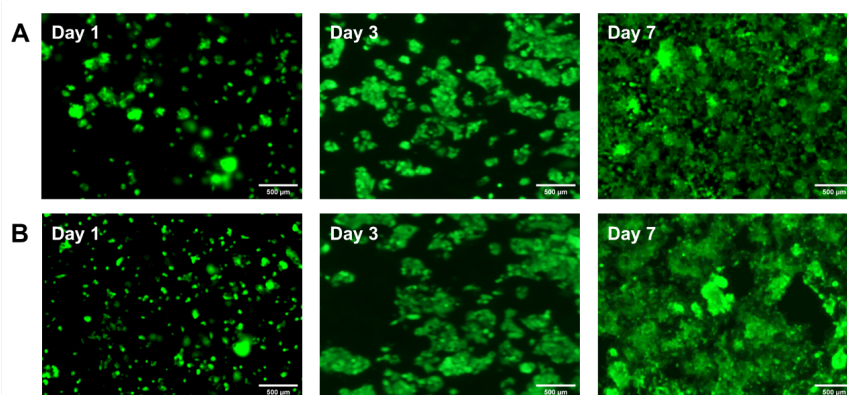


Figure 4. HepG2 cell viability study. The hepatocytes viability was assessed by using live/dead assay over a period of 7 days. (A) Control is HepG2 cells not exposed to electrodes (B) Test is HepG2 cells exposed to Nafion/MWCNT/GOx coated electrodes.

HepG2 cells are human nontumorigenic hepatoma cells that are most commonly used for drug metabolism and toxicity studies (39). Before using the designed glucose sensor for the LOC platform, we used the glucose sensor for 2D cell culture to evaluate the cytotoxicity of the biosensor. We cultured HepG2 cells in 2D for evaluation. A live/dead experiment was conducted using a solution containing D-PBS, calcein-AM, and Ethd-1. The living cells were dyed green due to calcein-AM, and the dead cells were dyed red due to Ethd-1. As can be seen from Fig. 4, for both the control well cultured under standard cell culture conditions and the test well coated with Nafion/MWCNT/GOx, very few red cells were found, and there was no difference in the cell survival rate in the live/dead assay.

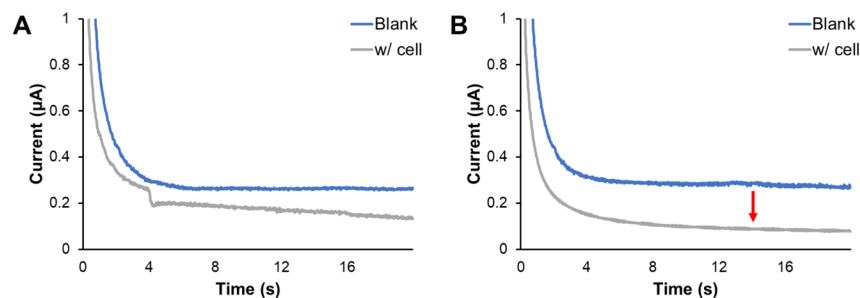


Figure 5. 3D cell culture glucose test. Cells consumed glucose in the cell culture medium through the decrease in the current of the w/ cell over time. (A: Day 1, B: Day 2)

Furthermore, to assess the applicability of the fabricated biosensor for the LOC platform 3D-bioprinted with hydrogels, we performed the glucose readout test by using HepG2 cells in 3D hydrogels. First, the hydrogel-containing cells were printed, and HepG2 cells were cultured with DMEM to conduct a current test. DMEM, the medium of the cell, contained 4.5 g/L of glucose and approximately 17.5–25 mM of glucose; the blank value was obtained similarly (Figure 3). However, as cells metabolized and consumed glucose contained in the medium, the concentration of glucose in the medium decreased. The current measurement of the medium in the hydrogel revealed that the current decreased more reliably on Day 2 than on Day 1 (Fig. 5), indicating that an electrode coated with Nafion/MWCNT/GOx can be used to measure the concentration of glucose remaining in the medium as the cells consume glucose, avoiding electrochemical interference with the interference material contained in the cells and the medium.

3.4. Fabrication of Liver-on-a-chip

We used a nonconductive PLA as the printing bioink for the LOC platform. The chip platform was printed on a sterilized glass slide. The PLA-based chip platform was then used for developing a bioprinted liver model by using a coaxial nozzle by directly extruding the HepG2 mixed collagen–alginate bioink from the outer nozzle and gelatin bioink from the inner nozzle. When the LOC was incubated at 37°C, the sacrificial material, that is, gelatin, which lined the inner core region of the construct, dissolved and flowed out, resulting in a lumen-based structure. The longitudinal and cross-sectional images of the LOC with stained hepatocytes are shown in Fig 6. As can be seen in the cross-sectional image, the core/shell model exhibited lumen-based structure formation. Thus, by using the coaxial bioprinting process, a core/shell 3D structure containing an empty tubular passage surrounded by hepatocyte plates that closely resemble the physiological unit of the liver sinusoid was fabricated.

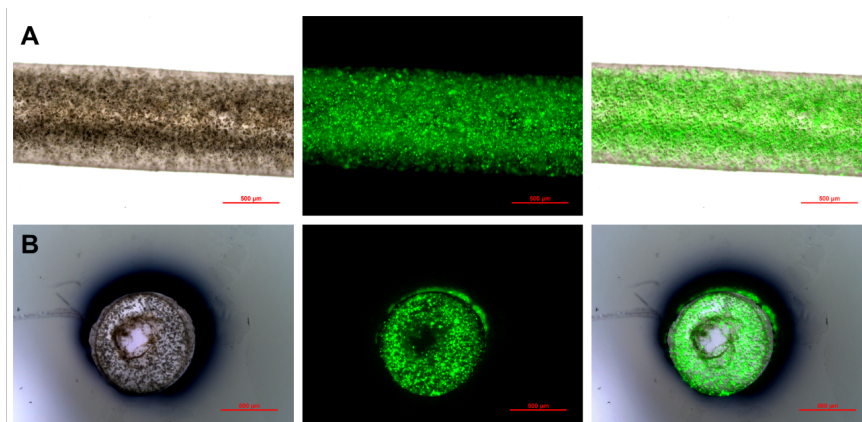


Figure 6. Fluorescence-based imaging of the hepatocyte-encapsulated 3D core/shell model. The LOC was stained with calcein-AM. (A) Microscopic image shows the longitudinal section and (B) cross-sectional view of the LOC with encapsulated hepatocytes. The cross-sectional view confirms the formation of the core/shell model of the LOC.

3.5. Cell proliferation of bioprinted LOC and drug response

The growth of hepatocytes on the LOC was determined using the CCK-8 proliferation assay kit over a period of 10 days. The graphical data of hepatocyte proliferation as percentage O.D. increase are shown in Fig. 7A. An increased hepatocyte proliferation rate was observed during the initial 7 days; the number of cells increased approximately tenfold. Post day 7, the proliferative capability reduced, and the growth of hepatocytes saturated. The considerable increase in the initial cell numbers was due to the abundant availability of medium and diffused gases throughout the in-vitro model as well as sufficient space for cellular growth and proliferation. This rapid increase in cell numbers during the first week reduced the per-cell-volume availability of medium components and diffused gases, inhibiting the cell growth cycle and resulting in increased cell necrosis. Furthermore, due to the overcrowding of cells, cell-cell contact inhibition occurred, which restricted cellular proliferation.

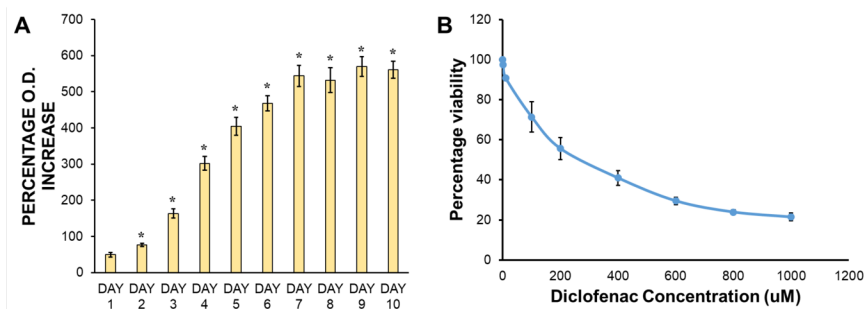


Figure 7. (A) The graphical data represents the percentage increase in WST-8 reduction through calorimetric measurements performed at 450 nm. The percentage increase in O.D. illustrates the number of viable hepatocytes in the LOC over a period of 10 days. (* $p < 0.05$) (B) Viability studies on the LOC platform for various concentrations of diclofenac over a period of 48 h.

To determine the toxic sensitivity of our fabricated 3D in vitro model, we performed a drug-toxicity test on the LOC (Fig. 7B). DF is a widely used anti-inflammatory drug. Multiple studies have reported that DF overdose causes liver toxicity and failure. We performed a cellular viability drug-toxicity test to study the dose-dependent drug toxicity on the hepatocytes in the LOC. LOC treatment with 1000 μM of DF exhibited a hepatocyte viability of 20%, indicating the acute toxicity of the drug at this concentration range. At a concentration of 100 μM , the percentage viability increased up to 70%, whereas the viability was more than 90% in the DF concentration below 10 μM . These results demonstrate that the developed LOC model is sensitive and has an improved hepatotoxic prediction over a wide range of drug concentrations.

3.6. Biosensor integration of LOC and glucose concentration measurement after drug test

The designed LOC platform includes two external medium blocks on both sides of the chip and a central space for holding the 3D-printed liver in-vitro model. The external medium blocks serve two purposes: (1) it allows the free movement of the medium through the hollow lumen of the 3D model, simulating a perfusion-based liver in-vitro model, and (2) it provides space for the easy placement and removal of biosensors onto the LOC. In OOC development, chip and sensor integration is a crucial task for eliminating various complex intermediate processes, such as enabling real-time cell monitoring. Extensive research has been conducted on OOC and sensor integration in recent years; however, few studies have used CP as a sensor for integration with the chip. Therefore, in this study, we have integrated 3D printed glucose biosensor and bioprinted

liver-on-a-chip to determine the accuracy and sensitivity of the fabricated CP-based electrode coated with Nafion/MWCNT/GOx.

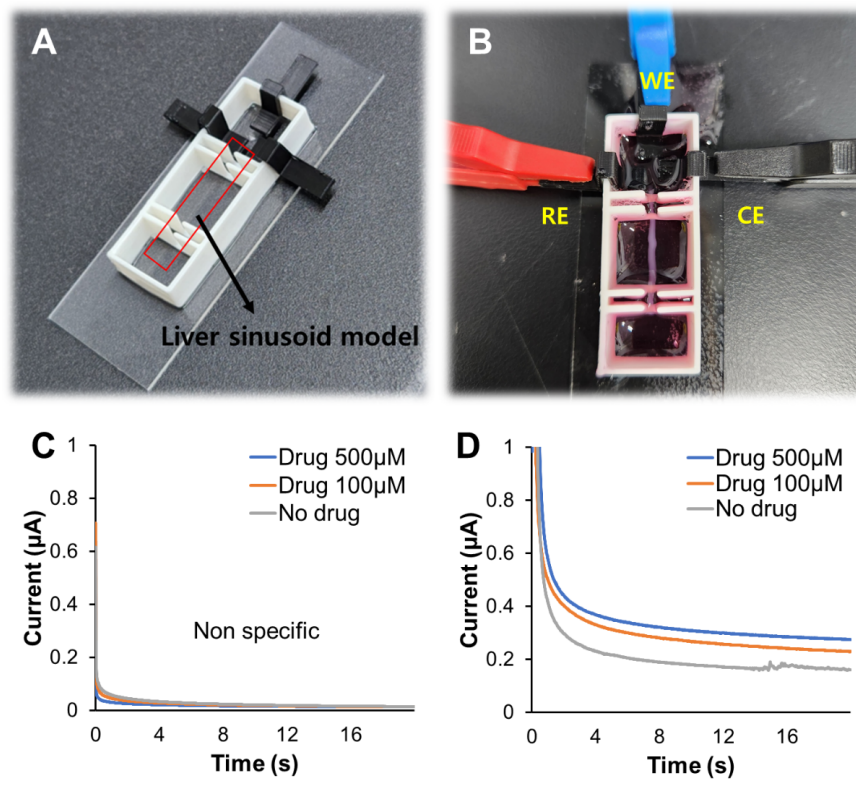


Figure 8. Biosensor integration with LOC. (A) Schematic diagram describing how to measure glucose in DMEM (B) The three-electrode system (working, reference, and counter electrodes) integrated with the LOC is connected to the potentiostat for performing cyclic voltammetry measurements. (C) & (D) Glucose measurement after drug tests (C: Nafion/GOx, D: Nafion/MWCNT/GOx).

To verify the sensitivity of the developed biosensor, a chronoamperometry analysis of the biosensor-integrated LOC was performed by subjecting it to treatment with two concentrations of DF (500 and 100 μM). The graphical data of current versus time are shown in Figure 8C and D. The Nafion/MWCNT/GOx-coated electrodes exhibited higher sensitivity compared to Nafion/GOx-coated electrodes, except for MWCNT, and a higher current was detected in the DF-treated LOC compared with the untreated LOC. As observed in the previous section (Figure 5), cells consume the glucose contained in the medium; thus, if cells are killed by drugs, glucose concentration should be reduced accordingly. However, as can be seen in Figure 8C, without MWCNT, all three graphs were similar, indicating the formation of non-specific graphs. In contrast, the higher current flow in Figure 8D directly indicated the presence of a high level of glucose in the medium due to cell death caused by the drug, resulting in a lesser amount of glucose being utilized by the resident cells. Among the drug-treated LOCs, a higher current flow was observed in the case of 500 μM DF treatment, which indicates a higher degree of cell death in this drug concentration range. Therefore, it can be concluded that the developed Nafion/MWCNT-based glucose biosensor is sensitive enough to detect minor changes in glucose concentration and has potential applications as an easily integratable OOC system.

Conclusion

In this study, we developed a portable, low-cost, and simple glucose monitoring device using a conductive PLA-based three-electrode electrochemical sensing system, which can be easily integrated with the OOC

platform. The glucose sensor was fabricated using the FDM method, and the electrode surface was modified by coating it with Nafion/MWCNT composites to improve its stability and biocompatibility. To determine the sensitivity of the glucose biosensing device, we bioprinted a perfusion-based liver-on-a-chip (LOC) platform. The biological characterization of the LOC demonstrated the proliferation of hepatocytes along with the expression of all liver-specific genes. Finally, a drug-toxicity study of the LOC biosensor device was performed, which demonstrated its ability to measure a broad range of glucose concentrations.

Acknowledgments

This work was supported by the National Research Foundation of Korea (NRF) grant funded by the Korean government (MSIT) (No. 2020R1C1C1011147).

Conflict of interest statement

The authors declare no commercial or financial conflict of interest.

References

1. Underhill, G.H., Peter, G., Chen, C.S. and Bhatia, S.N., (2012). Bioengineering methods for analysis of cells in vitro. *Annual review of cell and developmental biology* , 28 , p.385.
2. Mehling, M., (2014). Tay S. Microfluidic cell culture. *Curr Opin Biotechnol* , 25 , pp.95-102.
3. Esch, E.W., Bahinski, A. and Huh, D., (2015). Organs-on-chips at the frontiers of drug discovery. *Nature reviews Drug discovery* , 14 (4), pp.248-260.
4. Kimura, H., Yamamoto, T., Sakai, H., Sakai, Y. and Fujii, T., (2008). An integrated microfluidic system for long-term perfusion culture and on-line monitoring of intestinal tissue models. *Lab on a Chip* , 8 (5), pp.741-746.
5. Kim, H.J., Huh, D., Hamilton, G. and Ingber, D.E., (2012). Human gut-on-a-chip inhabited by microbial flora that experiences intestinal peristalsis-like motions and flow. *Lab on a Chip* , 12 (12), pp.2165-2174.
6. Wu, M.H., Huang, S.B. and Lee, G.B., (2010). Microfluidic cell culture systems for drug research. *Lab on a Chip* , 10 (8), pp.939-956.
7. Huh, D., Hamilton, G.A. and Ingber, D.E., (2011). From 3D cell culture to organs-on-chips. *Trends in cell biology* , 21 (12), pp.745-754.
8. Marx, U., Andersson, T.B., Bahinski, A., Beilmann, M., Beken, S., Cassee, F.R., Cirit, M., Daneshian, M., Fitzpatrick, S., Frey, O. and Gaertner, C., (2016). Biology-inspired microphysiological system approaches to solve the prediction dilemma of substance testing. *Alterx* , 33 (3), p.272.
9. Morgan, S.J., Elangbam, C.S., Berens, S., Janovitz, E., Vitsky, A., Zabka, T. and Conour, L., (2013). Use of animal models of human disease for nonclinical safety assessment of novel pharmaceuticals. *Toxicologic pathology* , 41 (3), pp.508-518.
10. Vinci, M., Gowan, S., Boxall, F., Patterson, L., Zimmermann, M., Lomas, C., Mendiola, M., Hardisson, D. and Eccles, S.A., (2012). Advances in establishment and analysis of three-dimensional tumor spheroid-based functional assays for target validation and drug evaluation. *BMC biology* , 10 (1), pp.1-21.
11. Cheah, L.T., Dou, Y.H., Seymour, A.M.L., Dyer, C.E., Haswell, S.J., Wadhawan, J.D. and Greenman, J., (2010). Microfluidic perfusion system for maintaining viable heart tissue with real-time electrochemical monitoring of reactive oxygen species. *Lab on a Chip* , 10 (20), pp.2720-2726.
12. Kieninger, J., Weltin, A., Flamm, H. and Urban, G.A., (2018). Microsensor systems for cell metabolism—from 2D culture to organ-on-chip. *Lab on a Chip* , 18 (9), pp.1274-1291.
13. Probst, C., Schneider, S. and Loskill, P., (2018). High-throughput organ-on-a-chip systems: Current status and remaining challenges. *Current Opinion in Biomedical Engineering* , 6 , pp.33-41.
14. Rogal, J., Probst, C. and Loskill, P., (2017). Integration concepts for multi-organ chips: how to maintain flexibility?!. *Future science OA* , 3 (2), p.FSO180.
15. Oomen, P.E., Skolimowski, M.D. and Verpoorte, E., (2016). Implementing oxygen control in chip-based cell and tissue culture systems. *Lab on a chip* , 16 (18), pp.3394-3414.

16. Brennan, M.D., Rexus-Hall, M.L., Elgass, L.J. and Eddington, D.T., (2014). Oxygen control with microfluidics. *Lab on a Chip* ,14 (22), pp.4305-4318.
17. Polini, A., Prodanov, L., Bhise, N.S., Manoharan, V., Dokmeci, M.R. and Khademhosseini, A., (2014). Organs-on-a-chip: a new tool for drug discovery. *Expert opinion on drug discovery* , 9 (4), pp.335-352.
18. Weise, F., Fernekorn, U., Hampl, J., Klett, M. and Schober, A., (2013). Analysis and comparison of oxygen consumption of HepG2 cells in a monolayer and three-dimensional high density cell culture by use of a matrigid®. *Biotechnology and Bioengineering* ,110 (9), pp.2504-2512.
19. Zhang, Y.S., Aleman, J., Shin, S.R., Kilic, T., Kim, D., Mousavi Shaegh, S.A., Massa, S., Riahi, R., Chae, S., Hu, N. and Avci, H., (2017). Multisensor-integrated Organs-On-Chips Platform for Automated and Continual. *Situ* .
20. Shah, P., Fritz, J.V., Glaab, E., Desai, M.S., Greenhalgh, K., Frachet, A., Niegowska, M., Estes, M., Jäger, C., Seguin-Devaux, C. and Zenhausern, F., (2016). A microfluidics-based in vitro model of the gastrointestinal human–microbe interface. *Nature communications* , 7 (1), pp.1-15.
21. Domansky, K., Inman, W., Serdy, J., Dash, A., Lim, M.H. and Griffith, L.G., (2010). Perfused multiwell plate for 3D liver tissue engineering. *Lab on a Chip* , 10 (1), pp.51-58.
22. McKenzie, J.R., Cognata, A.C., Davis, A.N., Wikswo, J.P. and Cliffel, D.E., (2015). Real-time monitoring of cellular bioenergetics with a multianalyte screen-printed electrode. *Analytical chemistry* ,87 (15), pp.7857-7864.
23. Curto, V.F., Marchiori, B., Hama, A., Pappa, A.M., Ferro, M.P., Braendlein, M., Rivnay, J., Fiocchi, M., Malliaras, G.G., Ramuz, M. and Owens, R.M., (2017). Organic transistor platform with integrated microfluidics for in-line multi-parametric in vitro cell monitoring. *Microsystems & nanoengineering* , 3 (1), pp.1-12.
24. Pohanka, M., (2016). Three-dimensional printing in analytical chemistry: principles and applications. *Analytical Letters* ,49 (18), pp.2865-2882.
25. Palenzuela, C.L.M. and Pumera, M., (2018). (Bio) Analytical chemistry enabled by 3D printing: Sensors and biosensors. *TrAC Trends in Analytical Chemistry* , 103 , pp.110-118.
26. Ambrosi, A. and Pumera, M., (2016). 3D-printing technologies for electrochemical applications. *Chemical Society Reviews* ,45 (10), pp.2740-2755.
27. Cardoso, R.M., Mendonça, D.M., Silva, W.P., Silva, M.N., Nossol, E., da Silva, R.A., Richter, E.M. and Muñoz, R.A., (2018). 3D printing for electroanalysis: From multiuse electrochemical cells to sensors. *Analytica chimica acta* , 1033 , pp.49-57.
28. Honeychurch, K.C., Rymansaib, Z. and Iravani, P., (2018). Anodic stripping voltammetric determination of zinc at a 3-D printed carbon nanofiber–graphite–polystyrene electrode using a carbon pseudo-reference electrode. *Sensors and Actuators B: Chemical* ,267 , pp.476-482.
29. Rymansaib, Z., Iravani, P., Emslie, E., Medvidović-Kosanović, M., Sak-Bosnar, M., Verdejo, R. and Marken, F., (2016). All-polystyrene 3D-printed electrochemical device with embedded carbon nanofiber-graphite-polystyrene composite conductor. *Electroanalysis* , 28 (7), pp.1517-1523.
30. Manzanares Palenzuela, C.L., Novotny, F., Krupicka, P., Sofer, Z. and Pumera, M., (2018). 3D-printed graphene/poly(lactic acid) electrodes promise high sensitivity in electroanalysis. *Analytical chemistry* , 90 (9), pp.5753-5757.
31. O’Neil, G.D., Ahmed, S., Halloran, K., Janusz, J.N., Rodríguez, A. and Rodríguez, I.M.T., (2019). Single-step fabrication of electrochemical flow cells utilizing multi-material 3D printing. *Electrochemistry Communications* , 99 , pp.56-60
32. Katseli, V., Economou, A., & Kokkinos, C., (2019). Single-step fabrication of an integrated 3D-printed device for electrochemical sensing applications. *Electrochemistry Communications*, 103 , pp.100-103
33. Balasubramanian, K., & Burghard, M., (2006). Biosensors based on carbon nanotubes. *Analytical and Bioanalytical Chemistry*, 385 (3), pp.452-468
34. Katz, E., & Willner, I., (2004). Biomolecule-functionalized carbon nanotubes: Applications in nanobioelectronics. *ChemPhysChem*, 5 (8), pp.1084-1104.
35. Guiseppi-Elie, A., Lei, C., & Baughman, R. H., (2002). Direct electron transfer of glucose oxidase on carbon nanotubes. *Nanotechnology* , 13 (5), 559.

36. Lee, H., Hong, Y. J., Baik, S., Hyeon, T., & Kim, D. H., (2018). Enzyme-based glucose sensor: from invasive to wearable device. *Advanced healthcare materials* , 7 (8), 1701150.
37. Wang, J., (2008). Electrochemical glucose biosensors. *Chemical reviews* , 108 (2), pp.814-825.
38. Bruen, D., Delaney, C., Florea, L., & Diamond, D., (2017). Glucose sensing for diabetes monitoring: recent developments. *Sensors* ,17 (8), 1866.
39. Kammerer, S. and Kupper, J.H., (2018). Human hepatocyte systems for in vitro toxicology analysis. *Journal of Cellular Biotechnology* ,3 (2), pp.85-93.